

Depuration of a solitary ascidian depletes transient bacteria without altering microbiome alpha-diversity

Brenna Hutchings¹, Susanna López-Legentil¹, Lauren M. Stefaniak², Marie L. Nydam³, Patrick M. Erwin^{1,*}

¹Department of Biology & Marine Biology, and Center for Marine Science, University of North Carolina Wilmington, Wilmington, NC 28409, United States

²Department of Marine Science, Coastal Carolina University, Conway, SC 29528, United States

³Life Sciences Concentration, Soka University of America, Aliso Viejo, CA 92656, United States

*Corresponding author. E-mail: Center for Marine Science, 5600 Marvin K. Moss Lane, Wilmington, NC 28409, United States. E-mail: erwinp@uncw.edu

Editor: [Julie Olson]

Abstract

Depuration, or the process of clearing impurities from the gut, is commonly applied to marine food products due to its efficacy in removing human pathogens from shellfish and edible ascidians. Recent studies also reported that depuration of filter-feeding animals helped reduce transient bacteria and identify resident symbionts in gut microbiome studies. Here, we examined the impact of depuration on bacteria in the branchial sac, gut, and hepatic gland of the solitary ascidian *Pyura vittata*. Replicates were kept in filtered seawater for 4 days prior to dissection (aquaria-depuration) and compared to samples that were immediately processed following collection (wild-no depuration) and replicates kept in unfiltered seawater for 4 days (aquaria-control). 16S rRNA gene sequence analysis revealed no significant differences among ascidian sources for microbial alpha-diversity but significant shifts in beta-diversity. Depuration reduced the number of core bacteria markedly (66%–84%) across all body regions, and bacteria that remained postdepuration consisted of genera associated with enhanced host health and resilience within other marine symbioses. Our results suggest that microbial profiles obtained following depuration do not substantially differ from those of nondepurated animals, but depuration can help differentiate transient from core and resident taxa in complex host–microbiome symbioses.

Keywords: ascidian; branchial sac; gut; hepatic gland; microbiome; starvation

Introduction

Depuration is the practice of clearing impurities within the gut by exposing animals to clean water, commonly applied to shellfish before sale for consumption. This method was effective at purging oysters of poliovirus and *Escherichia coli* (Mitchell et al. 1966) and removing human enterovirus from clams (Liu et al. 1967). To protect consumer health more effectively, new technologies have also been incorporated into the depuration process by adding naturally derived antibiotic products (Buatong et al. 2024) to clean saltwater or using plasma-activated (Pandiscia et al. 2024) instead of UV-sterilized or filtered seawater. Modern studies have utilized 16S rRNA amplicon sequencing to explore the microbial communities within shellfish gut tissue, where both host-specific symbiotic bacteria and environmentally sourced bacteria, some of which could pose human health risks, co-occur. Depuration of host organisms prior to symbiont characterization can help distinguish resident (well-established in host tissue) and transient (temporarily acquired through filter-feeding) microbiome members. In a meta-analysis of gut microbiomes from the edible mussel *Mytilus edulis*, e.g. depurated mussels displayed significantly different amplicon sequence variant (ASV) composition, 75% fewer ASVs, and a 35% decrease in the Shannon index than those that were non-depurated (Griffin et al. 2023). Thus, it is evident that transient microbes acquired through the filter-feeding activity of shellfish can be significantly reduced via depuration, while the resident

microbes that are established within host tissues remain present following depuration.

Ascidians or sea-squirts (Phylum Chordata, Class Ascidiacea) are marine filter-feeding invertebrates that host complex microbiomes, with some species like *Halocynthia roretzi* farmed by the seafood industry in Japan and Korea. Similar to shellfish, depuration before sale is recommended to reduce health risks during consumption, especially of raw ascidians (Kim et al. 2017). In edible ascidians, depuration over 3 days has been shown to greatly decrease the concentration of *E. coli* and bacteriophages, at faster rates than observed in oysters or mussels (Kim et al. 2017). When starved over the course of 6 days, *H. roretzi* display reduced microbial diversity, with increases or decreases in abundances of particular bacterial taxa (Wei et al. 2020). Furthermore, identifying core microbial community members (those present in all individuals of a treatment) in starved and unstarved ascidians has provided insight into which microbes could be planktonic or biofilm-forming within *Ciona intestinalis* (Dishaw et al. 2014), allowing researchers to draw more nuanced conclusions than when only studying non-depurated ascidians.

Here we assessed the impact of depuration on microbiome composition within the branchial sac, gut, and hepatic gland of a Belizean ascidian. The hepatic gland (also called “digestive gland” or “liver diverticula”) has ultrastructure and function comparable to vertebrate liver cells (Ermak 1977, Shin et al. 2014) but is

Received 24 April 2025; revised 9 July 2025; accepted 29 July 2025

© The Author(s) 2025. Published by Oxford University Press on behalf of FEMS. This is an Open Access article distributed under the terms of the Creative Commons Attribution-NonCommercial License (<https://creativecommons.org/licenses/by-nc/4.0/>), which permits non-commercial re-use, distribution, and reproduction in any medium, provided the original work is properly cited. For commercial re-use, please contact reprints@oup.com for reprints and translation rights for reprints. All other permissions can be obtained through our RightsLink service via the Permissions link on the article page on our site—for further information please contact journals.permissions@oup.com.

only found near the stomach in the families Pyuridae and Molgulidae and should not be confused with the pyloric gland, which is a set of tubes around the intestine (Rocha 2011). While the impact of depuration on the ascidian gut has been documented (Dishaw et al. 2014, Wei et al. 2020), to our knowledge, this is the first study to characterize an ascidian hepatic gland microbiome and other internal ascidian body regions following depuration. Replicates of the solitary stolidobranch ascidian *Pyura vittata* (Stimpson 1852) were kept in filtered seawater for 4 days prior to dissection (aquaria-depuration) and compared to samples that were immediately processed following collection (wild-no depuration). The microbiomes of additional replicates held in aquaria with unimpeded feeding (aquaria-control) prior to processing were also characterized. We hypothesized that depurated ascidians would harbor significantly lower biodiversity and different microbiome compositions than nondepurated ascidians.

Materials and methods

Sample collection and experimental design

All *Pyura vittata* and seawater samples used in this study were collected in July 2023 via snorkeling from the dock at Carrie Bow Cay Field Station, Belize (16.8000° N, 88.0833° W). On 5th July 2023, three replicates of 500 ml of ambient, surface seawater were collected on-site and immediately filtered through a sterile 0.2- μ m mesh with a Nalgene® vacuum filtration system and then stored in RNAlater® until further processing. Seawater samples were collected to characterize the bacterioplankton communities at the sampling site. The salinity at the site was 36ppt, and the temperature was 29.7 °C. In addition, five individuals of *P. vittata* (wild-no depuration; Fig. 1A) were collected on 5th July and processed immediately. Seven additional individuals of *P. vittata* were collected on 6th July and maintained in experimental aquaria for 4 days prior to processing. Four animals were kept in separate 500-ml tanks with air stones, and each tank was partially submerged in flow-through seawater directly pumped from the collection site. The constant flow-through water surrounding the tanks kept the seawater within the tanks at an average temperature of 29.65 °C throughout the experiment, as indicated by daily measurements ranging from 29.6 °C to 29.8 °C taken with a digital thermometer. Seawater inside the tanks was filtered through a sterile 0.2- μ m mesh with a Nalgene® vacuum filtration system to remove microbial cells and potential food particles (Fig. 1C; aquaria-depuration) and changed every 24 h to remove any fecal pellets (Fig. 1D). One individual held in a depuration tank died ~12 h before processing (mucus encasing the animal's tunic, strong smell) and was excluded from analysis (Fig. S1A and B). The remaining two individuals (aquaria-control) were placed directly in the flow-through seawater trough, on opposite sides to prevent microbial exchange between the animals. Placement in the flow-through seawater trough allowed the animals to feed during the 4 experimental days and controlled for potential microbiome shifts independent of the depuration process. Sample processing was identical for all ascidians (aquaria-control, wild-no depuration, aquaria-depuration): animals were kept in unfiltered ambient seawater with menthol crystals for 3 h to relax the animals prior to dissecting each animal's branchial sac, gut (intestine, independent of stomach), and hepatic gland (Fig. 1B). Previous work has indicated that menthol exposure has no significant impact on microbial alpha- or beta-diversity metrics in ascidians (Hutchings et al. 2025). Branchial sac samples were stored in 100% ethanol for use in ascidian barcoding to expand the GenBank® library of 18S rRNA ascidian gene

sequences, and gut and hepatic gland samples were stored in RNAlater®. All samples were kept at -20 °C for long-term storage upon return to the USA.

Ascidian barcoding

DNA extractions of a piece of each animal's dissected branchial sac were performed following the manufacturer instructions for the DNeasy® Blood and Tissue Kit (QIAGEN), except for one additional step. Following cell lysis in a Thermomixer (56 °C, 350 r/m), 20 μ l of RNase (10 mg/ml) was applied to each sample. The primer set F16/R497 (Price et al. 2005) was used to amplify a fragment of the 18S rRNA gene. Polymerase chain reactions (PCRs) were completed using 0.5 μ l of the forward and reverse primer set, 11 μ l of PCR water, 12.5 μ l of MyTaq™ HS Red Mix, and 0.5 μ l of DNA. Reactions were as follows: 95 °C for 1 min; 35 cycles of 95 °C for 15 sec, 45 °C for 15 sec, 72 °C for 10 sec; 72 °C for 1 min; and a holding temperature of 4 °C and were performed on an Eppendorf® Mastercycler® Nexus X2.

PCR products were visualized with gel electrophoresis and purified using the QIAquick PCR Purification Kit (QIAGEN). Sequencing reactions were completed using 5.5- μ l PCR water, 1.0- μ l BigDye™ Terminator v.3, 2.0- μ l BigDye™ Buffer (x5 concentration), 0.5 μ l of the respective forward or reverse primers, and 1.0 μ l of purified PCR product. Reactions were as follows: 96 °C for 1 min; 25 cycles of 50 °C for 5 sec, 60 °C for 4 min, 96 °C for 10 sec; 50 °C for 5 sec; 60 °C for 4 min; and a holding temperature of 10 °C and were run on an Eppendorf® Mastercycler® Nexus X2. The BigDye™ XTerminator Purification Kit (Applied Biosystems) was used to clean PCR products before sequencing on an Applied Biosystems 3500 genetic analyzer available at the UNCW Center for Marine Science. Sequences were aligned in Geneious (v. R11, Biomatters, Auckland, New Zealand) and consensus sequences deposited in GenBank® (PV505516-PV505525). 18S rRNA gene sequences were identical (100% sequence identity; 407 bp) for all *P. vittata* individuals.

Microbiome characterization

DNA extractions from branchial sac and hepatic gland tissue and ambient seawater filters were performed using the DNeasy® Blood and Tissue Kit (QIAGEN). DNA from the gut samples was extracted using the DNeasy® PowerSoil® Pro Kit (QIAGEN) due to the kit's efficacy at extracting DNA from gut and feces samples. No significant differences in microbial diversity or structure have been documented between the kits when used for microbial analysis of ascidian tissue samples (Evans et al. 2018). A NanoDrop® One Spectrophotometer was used to quantify DNA extracts, and the V4 region of the 16S rRNA gene was amplified using the 515f/806r primers (Caporaso et al. 2011). PCR reactions contained 0.5 μ l of the forward and reverse primers, 11 μ l of PCR water, 12.5 μ l of MyTaq™ HS Red Mix, and 0.5 μ l of DNA, and reactions were as follows: 95 °C for 2 min; 35 cycles of 95 °C for 15 sec, 50 °C for 15 sec, 72 °C for 20 sec; 72 °C for 2 min; and a holding temperature of 10 °C on an Eppendorf® Mastercycler® Nexus X2. PCR products were visualized via gel electrophoresis before sending 50 μ l of high-quality DNA extracts to Zymo Research Corporation (Irvine, California, USA) for next-generation sequencing (Illumina® NextSeq™) of the V4 region of the 16S rRNA gene with custom primers designed by Zymo corresponding to the 515f-806r primer pair region.

Returned forward and reverse sequence pairs were made contiguous (resulting in a mean read length of 252 bp) and processed in the mothur software package (v.1.43.0; Schloss et al. 2009) to produce operational taxonomic units (OTUs) based on 97% se-

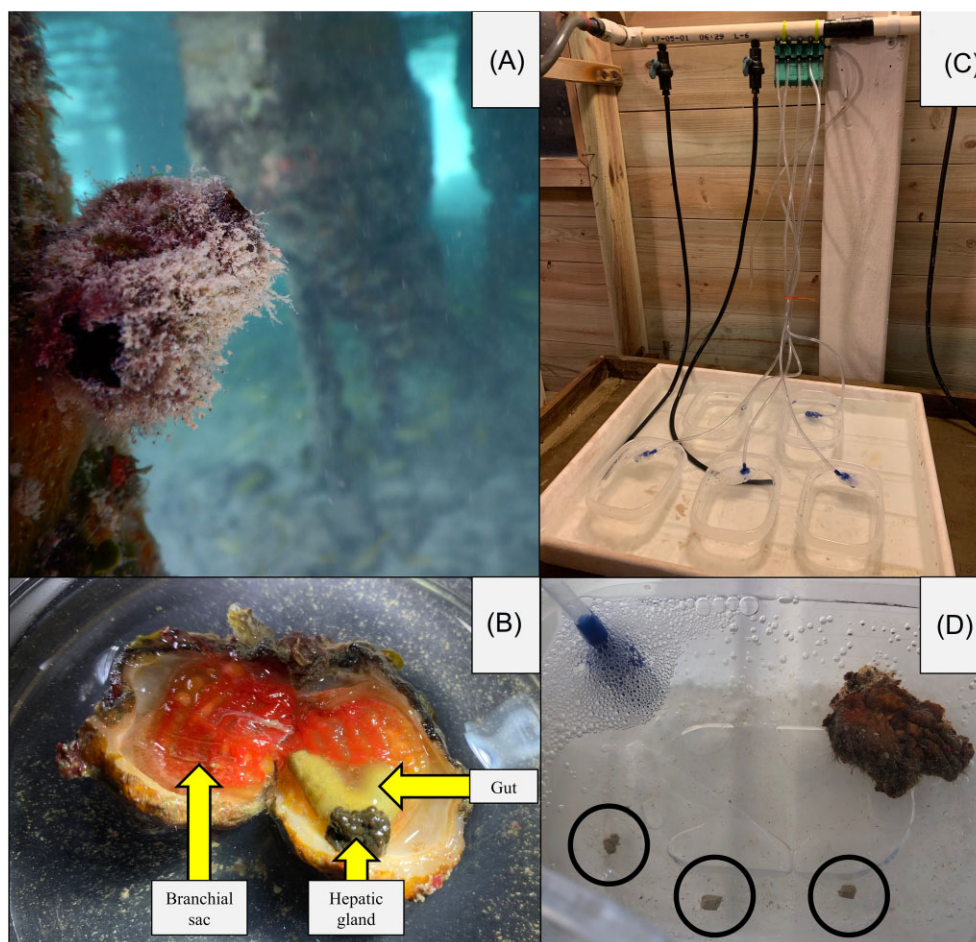


Figure 1 Individual of *P. vittata* in situ (A); dissection showing branchial sac (red), gut (green-brown), and hepatic gland (dark brown) body regions (B); five depuration tanks with air stones within flowing seawater trough (C); three fecal pellets (black circles) excreted by an individual within a depuration tank (D).

quence similarity. Sequences were aligned to the SILVA taxonomy database (v132.V4), OTUs were clustered *de novo*, rare OTUs (observed ≤ 5 times total in the entire dataset) were removed, and sequences were subsampled to the lowest sampling depth across all samples ($n = 25\,366$). A full bioinformatics pipeline, following Erwin et al. (2017), is available in Table S1. All samples from individual “5Jul23E,” one of the nondepurated ascidians, were excluded from processing due to the branchial sac from this animal having a low sequencing depth. Updated microbial taxa nomenclature (Oren et al. 2023) is used throughout this text, and raw 16S rRNA sequences have been deposited in NCBI SRA (PRJNA1218671).

Alpha- and beta-diversity

Alpha-diversity metrics (Shannon’s H' , richness, Pielou’s evenness) for the microbiome of all samples were calculated in R Studio (v2024.04.1+748). As the data were not normally distributed, a nonparametric Kruskal–Wallis test (`kruskal.test`, package “stats”) was completed to determine significance across samples by source (aquaria-control, wild-no depuration, aquaria-depuration, and seawater) or body region (branchial sac, gut, hepatic gland, and seawater). Post-hoc tests were completed using the pairwise Dunn test with Holm-adjusted P -values (`dunnTest`, package “FSA”) to determine significance between samples by source or body region. We also ran the nonparametric pairwise Dunn test to determine if there were any significant differences between sam-

ples by individual, as dictated by relatively low replication levels resulting from remote field logistics and replicate loss during processing (one ascidian died, another did not sequence well). Alpha-diversity metrics (Table S2) were visualized in box plots (`ggplot`, package “ggplot2”).

Beta-diversity was established using the Bray–Curtis dissimilarity, and to calculate significance across samples by source (aquaria-control, wild-no depuration, aquaria-depuration, seawater) or body region and the interaction of both factors the `adonis2` command in package “vegan” was utilized. Pairwise PERMANOVAs with FDR-adjusted P -values were calculated using the `adonis_pairwise` command from package `metagMisc` for source and body region, and beta dispersion was also calculated. A non-metric multidimensional scaling (nMDS) plot was created (`ggplot`, package “ggplot2”) to visualize beta-diversity.

OTU-level analysis

Core OTUs, defined here as OTUs shared among all individuals within a given source (aquaria-control, wild-no depuration, aquaria-depuration, seawater), were identified for the branchial sac, gut, and hepatic gland body regions. To identify OTUs that were significantly different between sample types based on exclusively source (pooling samples from all body regions) and exclusively body region (pooling samples from all sources), a multiple linear regression with covariate adjustment was run in Micro-

biomeAnalyst 2.0 (Chong et al. 2020) using the linear model option with FDR-adjusted *P*-values.

Results

Microbiome characterization

Quality filtering in mothur yielded 7 992 062 sequences (20.62% decrease in sequence count from the original 10 068 106 raw sequences) and subsampling 837 078 high-quality sequences (91.69% decrease from raw sequence count) that clustered into 13 435 OTUs. Archaea comprised 5.26% of all OTUs, with bacteria dominating all samples (Fig. S2). Pseudomonadota and Bacteroidota were the most abundant phyla across all sources (aquaria-control, wild-no depuration, aquaria-depuration, and seawater), but some samples were characterized by phyla that accounted for over 25% of their total read abundance (out of 25 366 sequences per sample): Fusobacteriota in the gut of 10Jul23E (37.48%), Epsilonbacteraeota in the branchial sac of 10Jul23E (38.58%), Planctomycetota in the branchial sac of 10Jul23B (37.89%), Patescibacteria in the branchial sac of 5Jul23A (35.86%), and Kiritimatiellota in the branchial sac of 5Jul23D (30.30%; Fig. 2). At the class level, Bacteroidia, Gamma-, and Alphaproteobacteria were present in high relative abundances across all sources, with the exception of the gut of 10Jul23E, of which Fusobacteriia was the most abundant class (37.48%; Fig. S3). At the level of order and lower, there was more interindividual variation in dominant taxa, but all samples were at least 25% composed of rare taxa ("other"; Figs. S4–S6).

Alpha- and beta-diversity

Since there were no significant differences between samples by individual for diversity, richness, or evenness (Table S3), all downstream analyses excluded "individual" as a factor. There were significant differences in microbial richness among samples from each source (aquaria-control, wild-no depuration, aquaria-depuration, seawater; $P = 0.018$; $X^2 = 10.022$) and from each body region ($P = 0.005$; $X^2 = 12.683$) but not in diversity or evenness (Table 1). These differences were driven entirely by distinctions between seawater and ascidian microbiomes (Table 2, Fig. 3). Pairwise comparisons based on source revealed that samples from aquaria-control ($P = 0.018$; $Z = -2.974$) and aquaria-depuration ($P = 0.026$; $Z = -2.790$) animals were significantly less rich than seawater samples (Fig. 3B). All other pairwise comparisons for alpha-diversity based on source were nonsignificant (Table 2; Fig. 3). Pairwise comparisons based on body region revealed that the branchial sac ($P = 0.022$; $Z = -2.844$) and hepatic gland ($P = 0.009$; $Z = -3.173$) samples were significantly less rich than seawater (Fig. 4B). All other pairwise comparisons for alpha-diversity by body region were nonsignificant (Table 2; Fig. 4).

PERMANOVAs revealed significant differences in microbial community composition across samples by source ($P = 0.001$; $R^2 = 0.213$; $F = 2.620$), body region ($P = 0.001$; $R^2 = 0.192$; $F = 2.301$), and between the two factors ($P = 0.001$; $R^2 = 0.417$; $F = 1.830$; Table 3). Pairwise PERMANOVAs revealed significant differences in microbial composition among all ascidian sources, and between all ascidian sources and seawater (Table 4). Beta dispersions indicated a homogenous (nonsignificant) dispersion between aquaria-control, aquaria-depuration, and wild-no depuration sources but were significant between seawater and ascidian samples ($P < 0.05$; Table 4). When considering the microbial composition in each body region, the only significant differences in pairwise comparisons were between ascidian tissues (branchial sac, gut, and hep-

atic gland) and seawater ($P < 0.05$), with beta dispersions displaying the same trend (Table 4). Visualized in the nMDS plot (stress = 0.088; Fig. 5), samples from the seawater communities were clustered separately from all ascidian samples (Fig. 5).

OTU-level analysis

For all body regions, aquaria-depuration decreased the number of core OTUs compared to the samples obtained from wild-no depuration individuals, by 69.49% in the branchial sac, 83.94% in the gut, and 66.67% in the hepatic gland (Table S4). Some core OTUs persisted in samples from both aquaria-depuration and wild-no depuration individuals and in all body regions (branchial sac, gut, and hepatic gland), with the gut being the tissue with the highest number of shared core OTUs (Fig. 6; Table S4).

The top five most abundant core OTUs were identified for each body region by source and across all samples from aquaria-control, aquaria-depuration, and wild-no depuration sources. Not all core OTUs in the wild-no depuration samples were classified as core in the aquaria-depuration samples, but they were still present in the ascidian tissues following depuration. Following depuration, members of the genera *Propionigenium* (#3) and *Synechococcus* CC9902 (#5) were no longer core to the branchial sac (Table 5) and were present in lower average abundances (64.31% and 95.85% decreases, respectively). *Arcobacter* (#4) was also no longer core to the branchial sac following depuration (Table 5) but had a 223.75% increase in abundance. In the gut, *Synechococcus* CC9902 (#5) was no longer core after depuration (Table 5) and had a 97.19% decrease in abundance. In the hepatic gland, *Ruegeria* (#15) was no longer core after depuration (Table 5) and had a 55.96% decrease in abundance, while members of family Rhodobacteraceae (#23), *Candidatus Nitrosopumilus* (#24), and *Pseudoalteromonas* (#27) were not core (Table 5) but had 60.99%, 26.76%, and 166.53% increases in average abundance.

There were other core OTUs that were shared across all samples of a given body region, regardless of source (aquaria-control, aquaria-depuration, and wild-no depuration). Only one core OTU (#1), a member of the bacterial genus *Catenococcus*, was detected in the branchial sac, gut, and hepatic gland samples from aquaria-control, aquaria-depuration, and wild-no depuration sources (Table 5). The most abundant core OTUs that were conserved in branchial sac samples from individuals in the aquaria-control, aquaria-depuration, and wild-no depuration sources were *Catenococcus* (#1), *Aestuariibacter* (#9), *Ruegeria* (#15), and *Thalassomonas* (#45; Table 5). For gut samples from the aquaria-control, aquaria-depuration, and wild-no depuration sources, the core OTUs were from the genera *Catenococcus* (#1), *Propionigenium* (#3), and *Arcobacter* (#4; Table 5). *Catenococcus* (#1) was the only core OTU in the hepatic gland samples from the aquaria-control, aquaria-depuration, and wild-no depuration sources (Table 5).

Differential abundance analysis of all OTUs revealed differences between ascidian and seawater microbiomes and fine-scale variability across ascidian sources. Ascidian samples had on average 5072.67 OTUs (37.76% of total) that were significantly different from OTUs retrieved for the seawater samples (Table S4). All ascidian samples had significantly lower abundances of order SAR11 (OTUs #16, 19) and family Cryomorphaceae (#21) members than the seawater samples (Table 6). In contrast, the number of OTUs that were significantly different among ascidian sources (aquaria-control, wild-no depuration, aquaria-depuration) accounted for less than 0.52% of the total OTUs in the dataset (Table S5). Similarly, between samples from different body regions, the number of significantly different OTUs was less than 0.48% of the total OTUs

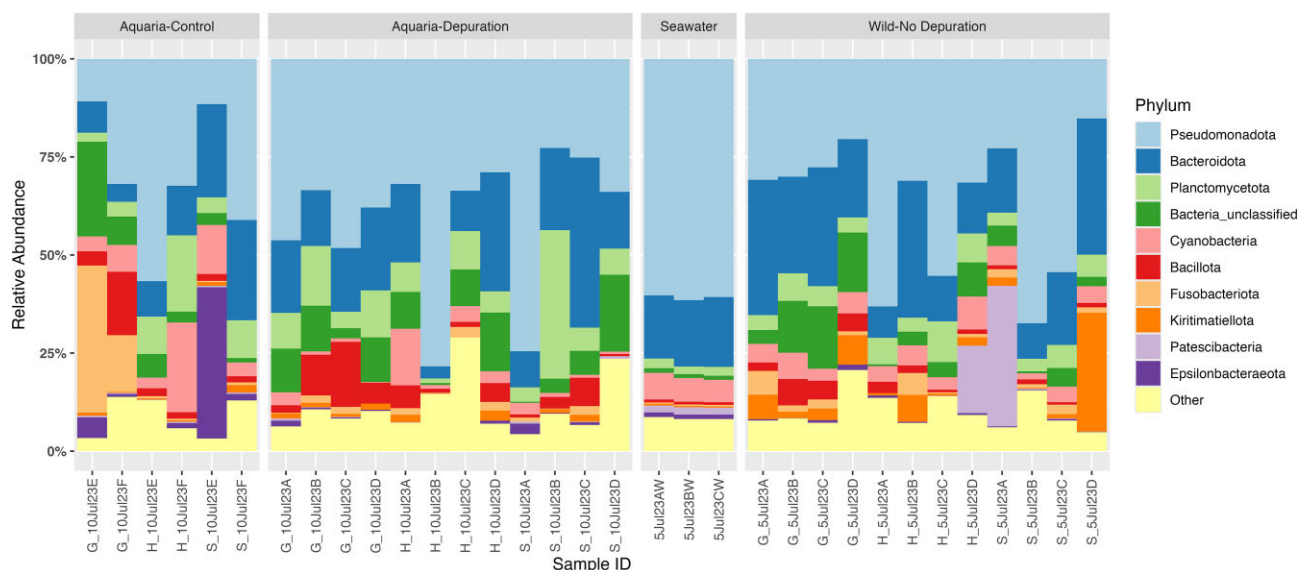


Figure 2 Stacked bar graphs of relative abundance of bacterial phyla within each sample. The top ten most abundant phyla within the dataset are shown, with all other phyla represented within the “Other” category. Samples are grouped by source and body region is indicated by the first letter of the corresponding “Sample ID”: branchial sac (S), gut (G), hepatic gland (H).

Table 1. Chi-squared (X^2) and P-values (P) for Shannon’s H’ diversity (Diversity), Richness, and Pielou’s evenness (Evenness) following the Kruskal–Wallis test across samples by source and body region.

Sample type	Diversity		Richness		Evenness	
	X^2	P	X^2	P	X^2	P
Source	5.434	0.143	10.022	0.018	0.201	0.978
Body region	7.491	0.058	12.683	0.005	4.676	0.197

Significant values are in bold.

Table 2. Z-values (Z), P-values (P), and Holm-adjusted P-values (P-adj) for Shannon’s H’ diversity (Diversity), Richness, and Pielou’s evenness (Evenness) following a Dunn test between samples by source: aquaria-control (Con), aquaria-depuration (Dep), wild-no depuration (No Dep), and seawater (SW); and body region: branchial sac (S), gut (G), hepatic gland (H).

Comparison	Diversity			Richness			Evenness		
	Z	P	P-adj	Z	P	P-adj	Z	P	P-adj
Con × Dep	−0.500	0.617	1.000	−0.603	0.546	0.546	−0.086	0.931	1.000
Con × No Dep	−0.793	0.428	1.000	−1.379	0.168	0.504	−0.034	0.973	0.973
Dep × No Dep	−0.359	0.720	0.712	−0.950	0.342	0.685	0.063	0.950	1.000
Con × SW	−2.243	0.025	0.150	−2.974	0.003	0.018	0.341	0.733	1.000
Dep × SW	−2.069	0.039	0.193	−2.790	0.005	0.026	0.441	0.660	1.000
No Dep × SW	1.842	0.065	0.262	2.190	0.029	0.114	−0.401	0.689	1.000
S × G	−1.503	0.133	0.531	−1.600	0.111	0.221	−0.185	0.853	1.000
S × H	−0.185	0.853	0.853	0.486	0.627	0.627	−1.919	0.055	0.330
G × H	1.318	0.187	0.375	2.081	0.037	0.150	−1.734	0.083	0.414
S × SW	−2.398	0.016	0.099	−2.844	0.004	0.022	−0.073	0.942	1.000
G × SW	−1.377	0.168	0.505	−1.760	0.078	0.235	0.052	0.958	0.958
H × SW	−2.273	0.023	0.115	−3.173	0.002	0.009	1.231	0.218	0.874

Significant values are in bold.

in the dataset (Table S5). Pairwise comparisons between samples from aquaria-depuration and wild-no depuration sources revealed significantly lower abundances of members of genus *Synechococcus* CC9902 (#5) and the family Desulfobacteraceae (#54) in aquaria-depuration and an increase in members of the genera *Alteromonas* (#17) and *Neptuniibacter* (#43; Table 6). Samples from animals in the aquaria-depuration source had greater abundances of *Alteromonas* (#17) and family Methanomicrobiaceae (#66), while

samples from the wild-no depuration source had more genus *Persicobacter* (#76; Table 6) bacteria than samples from aquaria-control.

Pairwise comparisons by body region revealed fine-scale differences among branchial sac, gut, and hepatic gland microbiomes. Branchial sac samples had significantly greater abundances of *Spirochaeta* 2 (#11) than gut samples, and significantly more *Endozoicomonas* (#84), *Nitrospira* (#174), and *SVA0996 Marine Group* (#441)

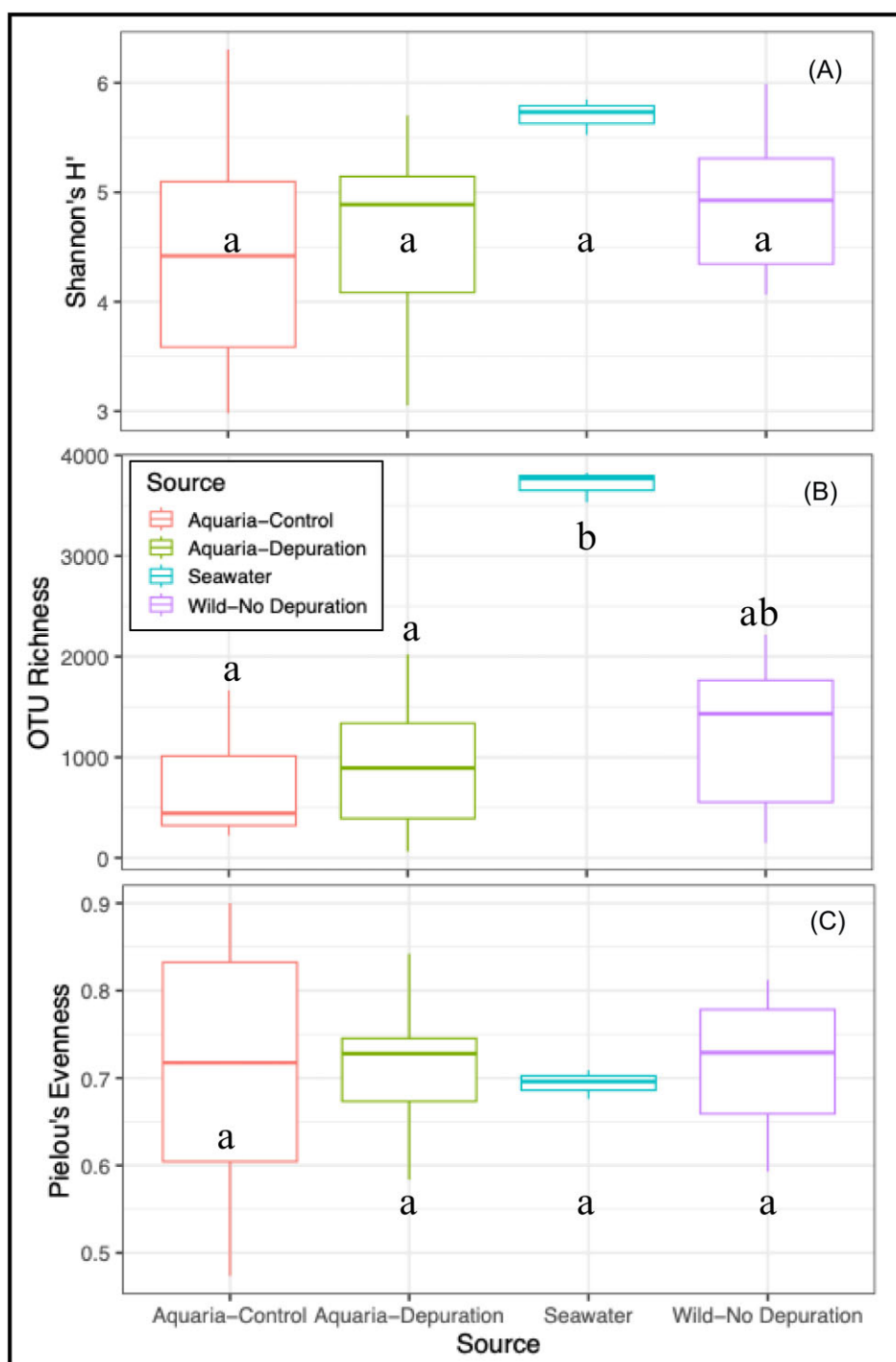


Figure 3 Boxplots of Shannon's H' diversity (A), richness (B), and Pielou's evenness (C) for samples by source. Dots show values 1.5 times the interquartile range. Lowercase letters indicate significant differences in alpha-diversity metrics between sample types.

Table 3. R^2 , F -statistic (F), and P -values (P) for PERMANOVAs calculated across samples by source and body region, and the interaction of factors.

Sample type	R^2	F	P
Source	0.213	2.620	0.001
Body region	0.192	2.301	0.001
Source \times body region	0.417	1.830	0.001

Significant values are in bold.

than hepatic gland samples (Table S6). Order Rickettsiales (#53) was significantly more abundant in branchial sac samples than gut or hepatic gland samples (Table S6). The genera *Halodesulfovibrio* (#62), *Pseudovibrio* (#67), and *Methanobrevibacter* (#89) were significantly more abundant in the gut than in the hepatic gland samples, and *Staphylococcus* (#18) was significantly more abundant in the gut than the branchial sac (Table S6). *Microbulbifer* (#79) was significantly more abundant in the gut than either the branchial sac or hepatic gland (Table S6).

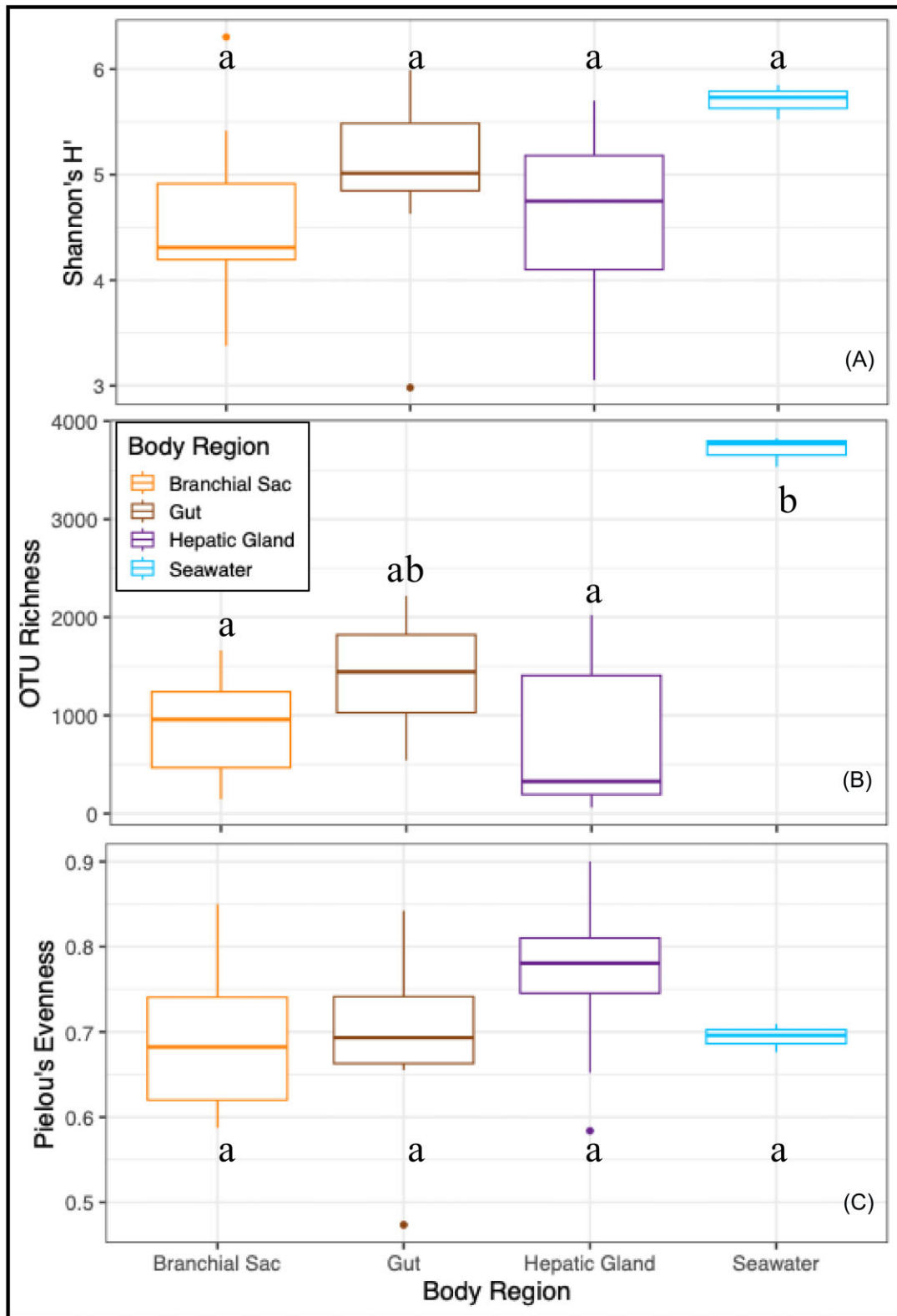


Figure 4 Boxplots of Shannon's H' diversity (A), richness (B), and Pielou's evenness (C) for samples by body region. Dots show values 1.5 times the interquartile range. Lowercase letters indicate significant differences in alpha-diversity metrics between sample types.

Table 4. R-squared (R^2), F-statistic (F), P-values (P), and FDR-adjusted P-values (P-adj) for pairwise PERMANOVAs calculated between samples by source: aquaria-control (Con), aquaria-depuration (Dep), wild-no depuration (No Dep), and seawater (SW), and body region: branchial sac (S), gut (G), and hepatic gland (H). P-values for beta dispersions (beta) and FDR-adjusted P-values for beta dispersions (beta-adj) are also reported.

Comparison	R^2	F	P	P-adj	Beta	Beta-adj
Con × Dep	0.080	1.400	0.037	0.037	0.624	0.624
Con × No Dep	0.105	1.870	0.008	0.016	0.371	0.445
Dep × No Dep	0.076	1.800	0.011	0.017	0.157	0.236
Con × SW	0.352	3.810	0.018	0.022	0.001	0.003
Dep × SW	0.241	4.126	0.002	0.006	0.001	0.003
No Dep × SW	0.278	5.017	0.002	0.006	0.003	0.006
S × G	0.075	1.453	0.040	0.060	0.137	0.182
S × H	0.052	0.989	0.423	0.423	0.868	0.868
G × H	0.073	1.465	0.063	0.076	0.152	0.182
S × SW	0.260	3.865	0.008	0.016	0.001	0.002
G × SW	0.315	5.047	0.004	0.012	0.001	0.002
H × SW	0.256	3.783	0.002	0.012	0.001	0.002

Significant values are in bold.

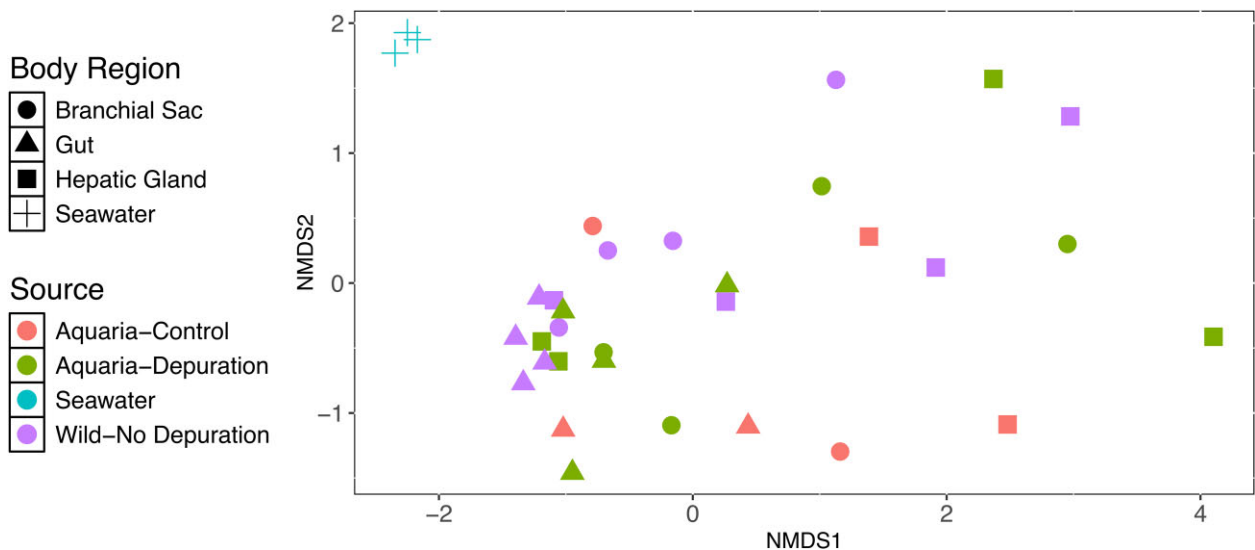


Figure 5 Nonmetric multidimensional scaling plot based on the Bray–Curtis similarity of microbial composition by the sample type. Source is denoted by color: aquaria-control (red), aquaria-depuration (olive green), wild-no depuration (purple), and seawater (blue). Body region is denoted by shape: branchial sac (circle), gut (triangle), hepatic gland (square), and seawater (cross). Stress for the plot is 0.088.

Discussion

Subjecting ascidians to a 4-day depuration resulted in no significant differences in microbiome diversity, richness, or evenness. However, the microbial composition of ascidians collected and analyzed immediately (wild-no depuration) differed significantly from those undergoing the 4-day depuration (aquaria-depuration). The branchial sac, gut, and hepatic gland of ascidians hosted microbial communities that were not significantly different in alpha- or beta-diversity. For all three body regions, the number of core OTUs was lower in aquaria-depuration samples than wild-no depuration samples, indicating that the depuration process can reduce the abundance of and/or remove transient microbes that could otherwise be mistaken as resident. In other ascidian species, depuration did not yield significant changes in either microbial alpha- or beta-diversity for the phlebobranch *C. intestinalis* (Dishaw et al. 2014), while significant differences in both metrics were found for the stolidobranch *H. roretzi* (Wei et al. 2020), suggesting that depuration may influence the microbiome differently depending on host species. Additionally, the amount of time

ascidians that are held in depuration tanks could change results, especially if the physiology of the animals is impacted as food limitation escalates to starvation. To our knowledge, the residence time of ingested material in *P. vittata* has not been established, so we selected a similar study design to that of Dishaw et al. (2014), with a duration of ca. 4 days and the use of 0.2- μ m filtered seawater. Over the course of our study, animals were observed producing feces up until the time they were removed from the depuration tanks, indicating that a starvation state had not yet been reached.

Here, we identified the core microbial taxa in the branchial sac, gut, and hepatic gland of *P. vittata*, expanding on data available for core microbes in the ascidian tunic (Erwin et al. 2013, López-Legentil et al. 2016, Evans et al. 2017, Dror et al. 2019, Casso et al. 2020, Galià-Camps et al. 2023), branchial sac (Galià-Camps et al. 2023), gut (Dishaw et al. 2014, Galià-Camps et al. 2023), and whole body (Murray et al. 2020, Liu et al. 2021). Moreover, we provide the first characterization of the microbes residing in the ascidian hepatic gland. The microbial communities in the hepatic gland samples were generally less rich (but not significantly so) than those

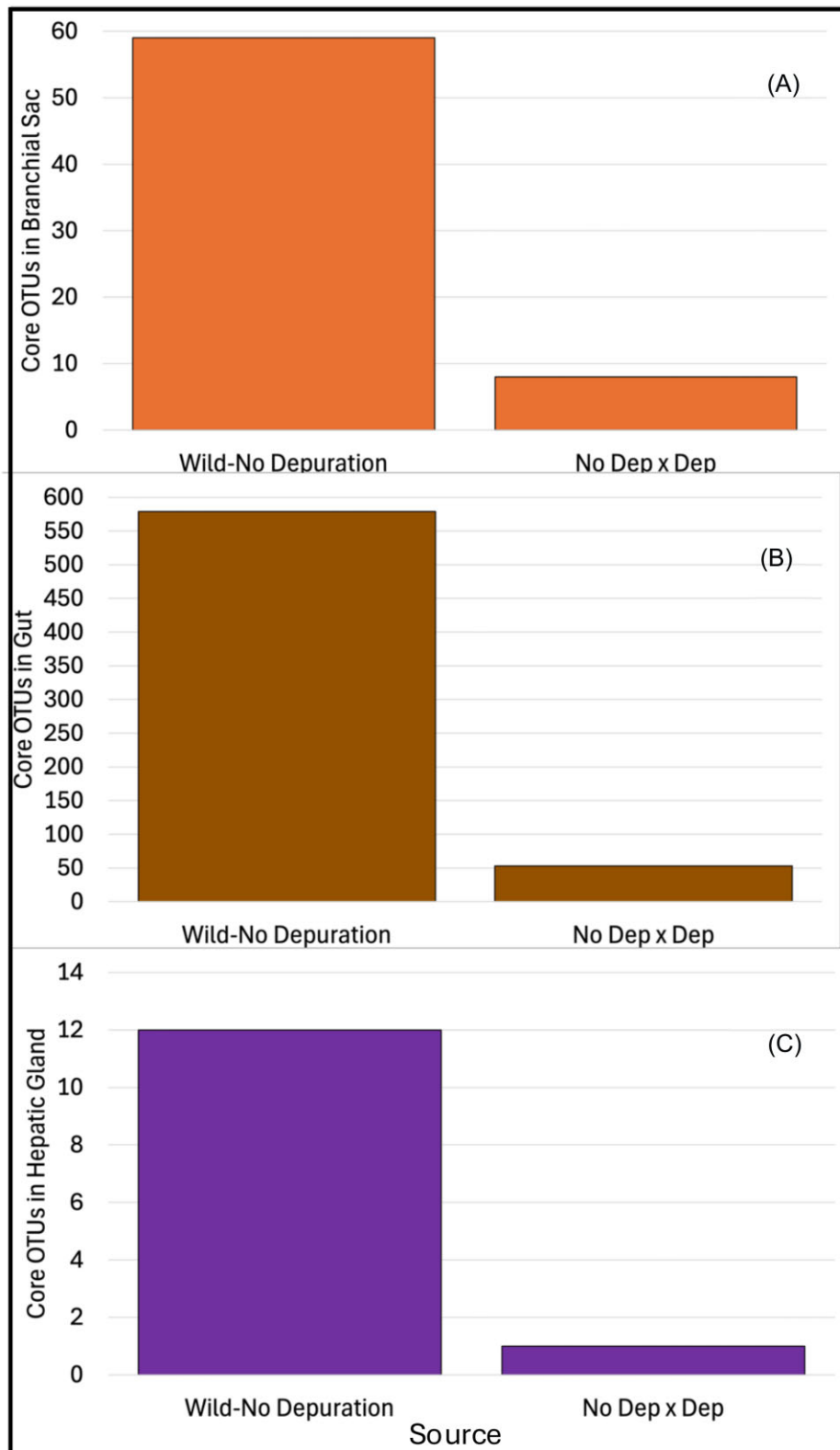


Figure 6 Bar graphs of the number of core OTUs within wild-no depuration and both aquaria-depuration and wild-no depuration sources for the branchial sac (A), gut (B), and hepatic gland (C) body regions.

Table 5. OTU number (#) and lowest known taxonomic identity of the top five most abundant core OTUs in aquaria-control (Con), wild-no depuration (No Dep), aquaria-depuration (Dep), and pairwise comparisons of these sources for branchial sac, gut, and hepatic gland body regions.

Source	Branchial sac		Gut		Hepatic gland	
	#	Identity	#	Identity	#	Identity
Con	1	<i>G. Catenococcus</i>	1	<i>G. Catenococcus</i>	1	<i>G. Catenococcus</i>
	2	<i>C. Bacteroidia</i>	2	<i>C. Bacteroidia</i>	2	<i>C. Bacteroidia</i>
	3	<i>G. Propionigenium</i>	3	<i>G. Propionigenium</i>	3	<i>G. Propionigenium</i>
	4	<i>G. Arcobacter</i>	4	<i>G. Arcobacter</i>	4	<i>G. Arcobacter</i>
	5	<i>G. Synechococcus</i> CC9902	5	<i>G. Synechococcus</i> CC9902	9	<i>G. Aestuariibacter</i>
No Dep	1	<i>G. Catenococcus</i>	1	<i>G. Catenococcus</i>	1	<i>G. Catenococcus</i>
	3	<i>G. Propionigenium</i>	2	<i>C. Bacteroidia</i>	15	<i>G. Ruegeria</i>
	4	<i>G. Arcobacter</i>	3	<i>G. Propionigenium</i>	23	<i>F. Rhodobacteraceae</i>
	5	<i>G. Synechococcus</i> CC9902	4	<i>G. Arcobacter</i>	24	<i>G. Candidatus Nitrosopumilus</i>
	9	<i>G. Aestuariibacter</i>	5	<i>G. Synechococcus</i> CC9902	27	<i>G. Pseudoalteromonas</i>
Dep	1	<i>G. Catenococcus</i>	1	<i>G. Catenococcus</i>	1	<i>G. Catenococcus</i>
	9	<i>G. Aestuariibacter</i>	2	<i>C. Bacteroidia</i>	3	<i>G. Propionigenium</i>
	15	<i>G. Ruegeria</i>	3	<i>G. Propionigenium</i>	40	<i>G. Roseimarinus</i>
	17	<i>G. Alteromonas</i>	4	<i>G. Arcobacter</i>	70	<i>G. Photobacterium</i>
	23	<i>F. Rhodobacteraceae</i>	7	<i>F. SM23-30 (Phycisphaerae)</i>		
Con × No Dep	1	<i>G. Catenococcus</i>	1	<i>G. Catenococcus</i>	1	<i>G. Catenococcus</i>
	3	<i>G. Propionigenium</i>	2	<i>C. Bacteroidia</i>	15	<i>G. Ruegeria</i>
	4	<i>G. Arcobacter</i>	3	<i>G. Propionigenium</i>	23	<i>F. Rhodobacteraceae</i>
	5	<i>G. Synechococcus</i> CC9902	4	<i>G. Arcobacter</i>	37	<i>G. Hoeflea</i>
	9	<i>G. Aestuariibacter</i>	5	<i>G. Synechococcus</i> CC9902	54	<i>F. Desulfobacteraceae</i>
Con × Dep	1	<i>G. Catenococcus</i>	1	<i>G. Catenococcus</i>	1	<i>G. Catenococcus</i>
	9	<i>G. Aestuariibacter</i>	2	<i>C. Bacteroidia</i>	3	<i>G. Propionigenium</i>
	15	<i>G. Ruegeria</i>	3	<i>G. Propionigenium</i>	70	<i>G. Photobacterium</i>
	23	<i>F. Rhodobacteraceae</i>	4	<i>G. Arcobacter</i>		
	45	<i>G. Thalassomonas</i>	7	<i>F. SM23-30 (Phycisphaerae)</i>		
No Dep × Dep	1	<i>G. Catenococcus</i>	1	<i>G. Catenococcus</i>	1	<i>G. Catenococcus</i>
	9	<i>G. Aestuariibacter</i>	2	<i>C. Bacteroidia</i>		
	15	<i>G. Ruegeria</i>	3	<i>G. Propionigenium</i>		
	23	<i>F. Rhodobacteraceae</i>	4	<i>G. Arcobacter</i>		
	25	<i>G. Shimia</i>	7	<i>F. SM23-30 (Phycisphaerae)</i>		
Con × No Dep × Dep	1	<i>G. Catenococcus</i>	1	<i>G. Catenococcus</i>	1	<i>G. Catenococcus</i>
	9	<i>G. Aestuariibacter</i>	2	<i>C. Bacteroidia</i>		
	15	<i>G. Ruegeria</i>	3	<i>G. Propionigenium</i>		
	23	<i>F. Rhodobacteraceae</i>	4	<i>G. Arcobacter</i>		
	45	<i>G. Thalassomonas</i>	7	<i>F. SM23-30 (Phycisphaerae)</i>		

Taxonomic ranks are abbreviated: Domain (D), Phylum (P), Class (C), Order (O), Family (F), Genus (G).

found in other body regions and primarily dominated by bacteria within the phyla Pseudomonadota and Bacteroidota. The hepatic gland also had the lowest number of core OTUs across all sources, indicating greater interindividual microbiome variability in this body region, with *Catenococcus* representing the only resident and core microbial taxon (OTU #1). Members of the genus *Catenococcus* have been identified as dominant bacteria within the gut of spiny lobsters (Amin et al. 2024), shrimp (Patil et al. 2021, Quintino-Rivera et al. 2023), and in coral mucus layers (Nguyen et al. 2023) and now in the hepatic gland of an ascidian. Further metagenomic work aiming to characterize functionality of the resident microbiome and additional studies of the hepatic gland (e.g. chemical and physiological investigations) in other ascidian species will reveal whether this particular genus contributes to glandular functions and if the microbial communities in the hepatic gland are host specific.

The gut of *P. vittata* contained the highest number of core bacteria compared to the branchial sac and hepatic gland regions, both before and after the depuration process. The most abundant gut bacterial taxa in both aquaria-depuration and wild-no depuration individuals likely represent resident microbes given their retention before and after depuration, and potential benefits

to the host ascidian. These included the aforementioned *Catenococcus* OTU (#1) and members of the genera *Propionigenium* and *Arcobacter*. The same taxa formed the core microbial communities in the gut of *C. intestinalis* individuals that were starved and unstarved (Dishaw et al. 2014), indicating specific associations of these bacteria with ascidian gut habitats and potential functionality within this niche. *Propionigenium* is dominant in the gut microbiome of sea urchins and known to aid in digestion (Hakim et al. 2019, Yao et al. 2019, Rodríguez-Barreras et al. 2021) and promote host health during stressful conditions (Ruiz-Barrionuevo et al. 2024). *Arcobacter* species are known to be pathogenic in some marine invertebrates like mussels (Li et al. 2018, 2019) and sea cucumbers (Zhao et al. 2019) but are innocuous and part of a routine microbiome in mud crabs (Wei et al. 2019), sea urchins (Hakim et al. 2019), and polychaetes (Hochstein et al. 2019). Thus, the ascidian gut microbiome is dominated by resident microbial taxa that are found in a variety of marine invertebrates and may have important roles in host animal health.

As found in the gut and hepatic gland microbiome, *Catenococcus* was an abundant core and resident OTU within the branchial sac (i.e. detected in both aquaria-depuration and wild-no depuration sources). Other OTUs present in branchial sac samples were affil-

Table 6. OTU number (#), lowest taxonomic identity (ID), P-value (P), FDR-adjusted P-value (P-adj), and average abundance based on sequence count per sample type of the top five most abundant OTUs that were significantly different between comparisons of source: aquaria-control (Con), aquaria-depuration (Dep), wild-no depuration (No Dep), and seawater (SW).

#	ID	P	P-adj	Average abundance			
				Con	Dep	No Dep	SW
17	Genus <i>Alteromonas</i>	3.51×10 ⁻³	0.03	4.33	382.33	0.17	11.33
66	Family Methanomicrobiaceae	4.61×10 ⁻³	0.04	1.33	101.75	30.25	0.00
200	Domain bacteria	5.01×10 ⁻³	0.04	0.00	34.75	16.75	0.00
378	Order NB1-j (Deltaproteobacteria)	3.42×10 ⁻³	0.03	30.67	1.75	0.75	0.00
421	Family Cellovibrionaceae	9.75×10 ⁻⁴	0.02	30.83	0.00	1.08	0.33
32	Order Bacteroidales	1.36×10 ⁻⁴	2.93×10 ⁻³	1.50	76.08	251.25	0.00
41	Class Gammaproteobacteria	2.10×10 ⁻³	0.02	460.00	0.92	0.17	0.33
61	Order Bacteroidales	1.41×10 ⁻⁵	3.20×10 ⁻⁴	1.00	13.42	230.67	0.00
76	Genus <i>Persicobacter</i>	8.90×10 ⁻⁵	1.95×10 ⁻³	0.00	38.75	130.58	5.67
86	Domain bacteria	5.99×10 ⁻³	4.74×10 ⁻²	10.17	35.42	107.92	0.00
2	Class Bacteroidia	3.06×10 ⁻³	0.01	524.83	714.17	1361.00	0.00
4	Genus <i>Arcobacter</i>	1.54×10 ⁻³	6.71×10 ⁻³	1972.00	51.92	56.17	1.67
7	Family SM23-30 (Phycisphaerae)	0.02	4.95×10 ⁻²	115.17	679.08	11.83	0.00
16	Family Clade II (SAR11)	1.50×10 ⁻²⁷	2.11×10 ⁻²⁵	0.83	0.25	0.00	2365.33
19	Genus Clade IA (SAR11)	4.93×10 ⁻¹⁶	2.21×10 ⁻¹⁴	0.83	2.58	1.75	2028.00
5	Genus <i>Synechococcus</i> CC9902	2.23×10 ⁻³	0.02	863.67	309.25	699.33	770.00
17	Genus <i>Alteromonas</i>	3.72×10 ⁻⁴	7.88×10 ⁻³	4.33	382.33	0.17	11.33
35	Class Bacteroidia	5.22×10 ⁻³	0.04	21.17	185.33	2.08	0.00
43	Genus <i>Neptuniibacter</i>	2.16×10 ⁻³	0.02	2.00	157.42	3.17	3.33
54	Family Desulfobacteraceae	5.63×10 ⁻⁴	0.01	63.50	57.67	180.25	13.33
5	Genus <i>Synechococcus</i> CC9902	0.01	0.03	863.67	309.25	699.33	770.00
16	Family Clade II (SAR11)	6.28×10 ⁻²⁹	9.63×10 ⁻²⁷	0.83	0.25	0.00	2365.33
19	Genus Clade IA (SAR11)	6.51×10 ⁻¹⁷	3.62×10 ⁻¹⁵	0.83	2.58	1.75	2028.00
21	Family Cryomorphaceae	6.84×10 ⁻⁵	5.08×10 ⁻⁴	30.50	24.08	35.58	1725.33
26	Genus <i>HIMB11</i> (Rhodobacteraceae)	5.86×10 ⁻⁴	4.13×10 ⁻³	2.50	17.50	416.50	693.67
1	Genus <i>Catenococcus</i>	0.01	0.03	556.67	1437.58	1420.42	246.33
2	Class Bacteroidia	2.61×10 ⁻³	8.94×10 ⁻³	524.83	714.17	1361.00	0.00
16	Family Clade II (SAR11)	5.02×10 ⁻²⁹	7.74×10 ⁻²⁷	0.83	0.25	0.00	2365.33
19	Genus Clade IA (SAR11)	6.58×10 ⁻¹⁷	3.65×10 ⁻¹⁵	0.83	2.58	1.75	2028.00
21	Family Cryomorphaceae	1.96×10 ⁻⁵	1.52×10 ⁻⁴	30.50	24.08	35.58	1725.33

Shaded cells indicate which sample types were compared.

iated with the genera *Aestuuriibacter*, *Ruegeria*, and *Thalassomonas*. *Aestuuriibacter* colonize plastics and have plastic (Morohoshi et al. 2018, Erni-Cassola et al. 2020, Al-Tarshi et al. 2024) and oil (Wang et al. 2014) degradation capabilities. *Aestuuriibacter* are also resistant to lead and cadmium (Zou et al. 2020) and can be obtained from the seawater by horizontal transmission (Giraud et al. 2021). *Ruegeria* are core members of the gut in multiple species of sea cucumber (Gao et al. 2022) and Pacific white shrimp (Amin et al. 2022) and have been associated with enhanced nutrient absorption (Huang et al. 2022) and the degradation of polystyrene (Zhao et al. 2024) in marine invertebrates. Strains of *Thalassomonas* have been isolated from abalone and sea anemone tissue (Hosoya et al. 2009) and display antimicrobial functions (Pheiffer et al. 2023). Thus, the core and resident bacterial taxa in *P. vittata* may play crucial roles in host health by processing pollutants, enhancing the immune response, and aiding in digestion, but metagenomic or metatranscriptomic studies are needed to determine the true function of resident bacteria within this species.

In conclusion, depuration of ascidians does not change microbial alpha-diversity profiles but may aid in differentiating transient from resident taxa in these complex microbiomes. Accordingly, analyses of nondepurated ascidians can yield similar microbiome profiles to those that have been depurated, in contrast to the disproportionately high alpha-diversity and significantly different microbial composition observed in other nondepurated filter-feeding invertebrates (e.g. mussels, Griffin et al. 2023). Resi-

dent microbial taxa are more likely to be functionally necessary for the host and participate in overall ascidian health and homeostasis, and studies targeting this fraction of the microbiome may benefit from depuration treatments. Ultimately, whether to subject ascidians to depuration prior to analysis should be informed by the objectives of each study and the amenability of the host organisms to depuration treatments.

Acknowledgments

We wish to thank the excellent staff at Carrie Bow Cay Field Station for their support in July of 2023. All samples were collected and exported with permission from the Belize Fisheries Department, Scientific Research Permit 0037–22. Support was provided by the Smithsonian Institute's Caribbean Coral Reef Ecosystems (CCRE) Program (contribution number 1073).

Author Contributions

Brenna Hutchings (Conceptualization, Formal Analysis, Investigation, Writing—original draft, Writing—review & editing), Susanna López-Legentil (Conceptualization, Formal Analysis, Funding acquisition, Investigation, Writing—original draft, Writing—review & editing), Lauren M Stefaniak (Funding acquisition), Marie L Nydam (Funding acquisition, Writing—review & editing), and Patrick Michael Erwin (Conceptualization, Formal Analysis, Funding ac-

quisition, Investigation, Writing – original draft, Writing—review & editing).

Supplementary data

Supplementary data is available at *FEMSEC Journal* online.

Conflicts of interest: Authors have no relevant financial or nonfinancial interests to declare.

Funding

This work was supported by the National Science Foundation (grant number DEB-2122475) and a Ruth D. Turner Foundation Scholarship in Marine Biology awarded to BH (2022).

References

- Al-Tarshi M, Dobretsov S, Al-Belushi M. Bacterial communities across multiple ecological niches (water, sediment, plastic, and snail gut) in mangrove habitats. *Microorganisms* 2024;**12**:1561. <https://doi.org/10.3390/microorganisms12081561>.
- Amin M, Kumala RRC, Mukti AT et al. Metagenomic profiles of core and signature bacteria in the guts of white shrimp, *Litopenaeus vannamei*, with different growth rates. *Aquaculture* 2022;**550**:737849. <https://doi.org/10.1016/j.aquaculture.2021.737849>.
- Amin M, Taha H, Musdalifah L et al. Structure and diversity of microbiome associated with the gastrointestinal tracts of wild spiny lobsters and profiling their potential probiotic properties using eDNA metabarcoding. *Fishes* 2024;**9**:264. <https://doi.org/10.3390/fishes9070264>.
- Buatong J, Bahem N, Benjakul S et al. Depuration of Asian green mussels using chitooligosaccharide-epigallocatechin gallate conjugate: shelf-life extension, microbial diversity, and quality changes during refrigerated storage. *Foods* 2024;**13**:3104. <https://doi.org/10.3390/foods13193104>.
- Caporaso JG, Lauber CL, Walters WA et al. Global patterns of 16 s rRNA diversity at a depth of millions of sequences per sample. *Proc Natl Acad Sci USA* 2011;**108**:4516–22. <https://doi.org/10.1073/pnas.1000080107>.
- Casso M, Turon M, Marco N et al. The microbiome of the worldwide invasive ascidian *Didemnum vexillum*. *Front Mar Sci* 2020;**7**:201. <https://doi.org/10.3389/fmars.2020.00201>.
- Chong J, Liu P, Zhou G et al. Using MicrobiomeAnalyst for comprehensive statistical, functional, and meta-analysis of microbiome data. *Nat Protoc* 2020;**15**:799–821. <https://doi.org/10.1038/s41596-019-0264-1>.
- Dishaw LJ, Flores-Torres J, Lax S et al. The gut of geographically disparate *Ciona intestinalis* harbors a core microbiota. *PLoS One* 2014;**9**:e93386. <https://doi.org/10.1371/journal.pone.0093386>.
- Dror H, Novak L, Evans JS et al. Core and dynamic microbial communities of two invasive ascidians: can host-symbiont dynamics plasticity affect invasion capacity? *Microb Ecol* 2019;**78**:170–84. <https://doi.org/10.1007/s00248-018-1276-z>.
- Ermak TH. Glycogen deposits in the pyloric gland of the ascidian *Styela clava* (Urochordata). *Cell Tissue Res* 1977;**176**:47–55. <https://doi.org/10.1007/BF00220343>.
- Erni-Cassola G, Wright RJ, Gibson MI et al. Early colonization of weathered polyethylene by distinct bacteria in marine coastal seawater. *Microb Ecol* 2020;**79**:517–26. <https://doi.org/10.1007/s00248-019-01424-5>.
- Erwin PM, Pineda MC, Webster N et al. Small core communities and high variability in bacteria associated with the introduced ascidian *Styela plicata*. *Symbiosis* 2013;**59**:35–46. <https://doi.org/10.1007/s13199-012-0204-0>.
- Erwin PM, Rhodes RG, Kiser KB et al. High diversity and unique composition of gut microbiomes in pygmy (*Kogia breviceps*) and dwarf (*K. sima*) sperm whales. *Sci Rep* 2017;**7**:7205. <https://doi.org/10.1038/s41598-017-07425-z>.
- Evans JS, Erwin PM, Shenkar N et al. Introduced ascidians harbor highly diverse and host-specific microbial assemblages. *Sci Rep* 2017;**7**:11033. <https://doi.org/10.1038/s41598-017-11441-4>.
- Evans JS, López-Legentil S, Erwin PM. Comparing two common DNA extraction kits for the characterization of symbiotic microbial communities from ascidian tissue. *Microbes Environ* 2018;**33**:435–9. <https://doi.org/10.1264/jsme2.ME18031>.
- Galià-Camps C, Baños E, Pascual M et al. Multidimensional variability of the microbiome of an invasive ascidian species. *iScience* 2023;**26**:107812. <https://doi.org/10.1016/j.isci.2023.107812>.
- Gao F, Zhang Y, Wu P et al. Bacterial community composition in gut content and ambient sediment of two tropical wild sea cucumbers (*Holothuria atra* and *H. leucospilota*). *J Ocean Limnol* 2022;**40**:360–72. <https://doi.org/10.1007/s00343-021-1001-5>.
- Giraud C, Callac N, Beauvais M et al. Potential lineage transmission within the active microbiota of the eggs and the nauplii of the shrimp *Litopenaeus stylirostris*: possible influence of the rearing water and more. *PeerJ* 2021;**9**:e12241. <https://doi.org/10.7717/peerj.12241>.
- Griffin TW, Darsan MA, Collins HI et al. A multi-study analysis of gut microbiome data from the blue mussel (*Mytilus edulis*) emphasises the impact of depuration on biological interpretation. *Environ Microbiol* 2023;**25**:3435–49. <https://doi.org/10.1111/1462-2920.16537>.
- Hakim JA, Schram JB, Galloway AWE et al. The purple sea urchin *Strongylocentrotus purpuratus* demonstrates a compartmentalization of gut bacterial microbiota, predictive functional attributes, and taxonomic co-occurrence. *Microorganisms* 2019;**7**:35. <https://doi.org/10.3390/microorganisms7020035>.
- Hochstein R, Zhang Q, Sadowsky MJ et al. The deposit feeder *Capitella teleta* has a unique and relatively complex microbiome likely supporting its ability to degrade pollutants. *Sci Total Environ* 2019;**670**:547–54. <https://doi.org/10.1016/j.scitotenv.2019.03.255>.
- Hosoya S, Adachi K, Kasai H. *Thalassomonas actiniarum* sp. nov. and *Thalassomonas haliotis* sp. nov., isolated from marine animals. *Int J Syst Evol Microbiol* 2009;**59**:686–90. <https://doi.org/10.1099/ijs.0.000539-0>.
- Huang L, Guo H, Liu Z et al. Contrasting patterns of bacterial communities in the rearing water and gut of *Penaeus vannamei* in response to exogenous glucose addition. *Mar Life Sci Technol* 2022;**4**:222–36. <https://doi.org/10.1007/s42995-021-00124-9>.
- Hutchings B, López-Legentil S, Stefaniak L et al. Microbial distortion? Impacts of delayed preservation on microbiome diversity and composition in a marine invertebrate. *MicrobiologyOpen* 2025;**14**:e70019. <https://doi.org/10.1002/mbo3.70019>.
- Kim JH, Shim KB, Shin SB et al. Comparison of bioaccumulation and elimination of *Escherichia coli* and male-specific bacteriophages by ascidians and bivalves. *Environ Sci Pollut Res* 2017;**24**:28268–76. <https://doi.org/10.1007/s11356-017-0736-1>.
- Li Y, Xu J, Chen Y et al. Characterization of gut microbiome in the mussel *Mytilus galloprovincialis* in response to thermal stress. *Front Physiol* 2019;**10**:1086. <https://doi.org/10.3389/fphys.2019.01086>.
- Li Y, Yang N, Liang X et al. Elevated seawater temperatures decrease microbial diversity in the gut of *Mytilus coruscus*. *Front Physiol* 2018;**9**:839. <https://doi.org/10.3389/fphys.2018.00839>.

- Liu OC, Seraichekas HR, Murphy BL. Viral depuration of the Northern Quahaug. *Appl Microbiol* 1967;**15**:307–15. <https://journals.asm.org/doi/10.1128/am.15.2.307-315.1967> (9 July 2025, date last accessed).
- Liu Y, Wu P, Li C et al. The bacterial composition associated with *Atrialum robustum*, a common ascidian from Xisha coral reef, China. *Symbiosis* 2021;**83**:153–61. <https://doi.org/10.1007/s13199-020-00742-4>.
- López-Legentil S, Turon X, Erwin PM. Feeding cessation alters host morphology and bacterial communities in the ascidian *Pseudodistoma crucigaster*. *Front Zool* 2016;**13**:2. <https://doi.org/10.1186/s12983-016-0134-4>.
- Mitchell JR, Presnell MW, Akin EW et al. Accumulation and elimination of poliovirus by the Eastern oyster. *AJE* 1966;**84**:40–50. <https://doi.org/10.1093/oxfordjournals.aje.a120626>.
- Morohoshi T, Ogata K, Okura T et al. Molecular characterization of the bacterial community in biofilms for degradation of poly(3-hydroxybutyrate-co-3-hydroxyhexanoate) films in seawater. *M&E* 2018;**33**:19–25.
- Murray AE, Avalon NE, Bishop L et al. Uncovering the core microbiome and distribution of palmerolide in *Synoicum adareanum* across the Anvers Island Archipelago, Antarctica. *Mar Drugs* 2020;**18**:298. <https://doi.org/10.3390/md18060298>.
- Nguyen DH, Bettarel Y, Chu HH et al. An analysis of the bacterial community in and around scleractinian corals of Phu Quoc Island, Vietnam. *Reg Stud Mar Sci* 2023;**60**:102817. <https://doi.org/10.1016/j.risma.2023.102817>.
- Oren A, Arahal DR, Göker M et al. International code of nomenclature of prokaryotes. Prokaryotic code (2022 revision). *Int J Syst Evol Microbiol* 2023;**73**:5585. <https://doi.org/10.1099/ijsem.0.005585>.
- Pandiscia A, Lorusso P, Manfredi A et al. Leveraging plasma-activated seawater for the control of human norovirus and bacterial pathogens in shellfish depuration. *Foods* 2024;**13**:850. <https://doi.org/10.3390/foods13060850>.
- Patil PK, Vinay TN, Ghate SD et al. 16S rRNA gene diversity and gut microbial composition of the Indian white shrimp (*Penaeus indicus*). *Antonie Van Leeuwenhoek* 2021;**114**:2019–31. <https://doi.org/10.1007/s10482-021-01658-9>.
- Pheiffer F, Schneider YKH, Hansen EH et al. Bioassay-guided fractionation leads to the detection of cholic acid generated by the rare *Thalassomonas* sp. *Mar Drugs* 2023;**21**:2. <https://doi.org/10.3390/md21010002>.
- Price A, Collie JS, Smith D. 18s ribosomal RNA and cytochrome oxidase gene sequences of *Didemnum* sp., an invasive colonial tunicate. SURFO Technical Report No. 2006-01:46-53. 2005. https://digitalcommons.uri.edu/cgi/viewcontent.cgi?article=1005&context=surfo_tech_reports#page=52 (9 July 2025, date last accessed).
- Quintino-Rivera JG, Elizondo-González R, Gamboa-Delgado J et al. Metabolic turnover rate, digestive enzyme activities, and bacterial communities in the white shrimp *Litopenaeus vannamei* under compensatory growth. *PeerJ* 2023;**11**:e14747. <https://doi.org/10.7171/peerj.14747>.
- Rocha R. Glossary of tunicate terminology—training in tropical taxonomy. *Smithsonian Tropical Research Institute* 2011. <https://striresearch.si.edu/taxonomy-training/resources/glossary-of-tunicate-terminology/> (9 July 2025, date last accessed).
- Rodríguez-Barreras R, Tosado-Rodríguez EL, Godoy-Vitorino F. Trophic niches reflect compositional differences in microbiota among Caribbean sea urchins. *PeerJ* 2021;**9**:e12084. <https://doi.org/10.7717/peerj.12084>.
- Ruiz-Barrionuevo JM, Kardas E, Rodríguez-Barreras R et al. Shifts in the gut microbiota of sea urchin *Diadema antillarum* associated with the 2022 disease outbreak. *Front Microbiol* 2024;**15**: 1409729. <https://doi.org/10.3389/fmicb.2024.1409729>.
- Schloss PD, Westcott SL, Ryabin T et al. Introducing mothur: open-source, platform-independent, community-supported software for describing and comparing microbial communities. *Appl Environ Microb* 2009;**75**:7537–41. <https://doi.org/10.1128/AEM.01541-09>.
- Shin YK, Park JJ, Myeong J et al. Digestive gland ultrastructure of the tunicate, *Halocynthia roretzi* (Ascidiacea: pyuridae) in relation to function. *JCLM* 2014;**2**:947–52. <https://doi.org/10.12980/JCLM.2.2014JCLM-2014-0090>.
- Stimpson W. Several new ascidians from the coast of the United States. *Proc Boston Soc Nat Hist* 1852;**4**:228–32.
- Wang W, Zhong R, Shan D et al. Indigenous oil-degrading bacteria in crude oil-contaminated seawater of the Yellow Sea, China. *Appl Microbiol Biotechnol* 2014;**98**:7253–69. <https://doi.org/10.1007/s00253-014-5817-1>.
- Wei H, Wang H, Tang L et al. High-throughput sequencing reveals the core gut microbiota of the mud crab (*Scylla paramamosain*) in different coastal regions of southern China. *Bmc Genomics [Electronic Resource]* 2019;**20**:829. <https://doi.org/10.1186/s12864-019-6219-7>.
- Wei J, Gao H, Yang Y et al. Seasonal dynamics and starvation impact on the gut microbiome of urochordate ascidian *Halocynthia roretzi*. *Anim Microbiome* 2020;**2**:30. <https://doi.org/10.1186/s42523-020-00048-2>.
- Yao Q, Yu K, Liang J et al. The composition, diversity and predictive metabolic profiles of bacteria associated with the gut digesta of five sea urchins in Luhuitou Fringing Reef (Northern South China Sea). *Front Microbiol* 2019;**10**:1168. <https://doi.org/10.3389/fmicb.2019.01168>.
- Zhao S, Liu R, Lv S et al. Polystyrene-degrading bacteria in the gut microbiome of marine benthic polychaetes support enhanced digestion of plastic fragments. *Commun Earth Environ* 2024;**5**:162. <https://doi.org/10.1038/s43247-024-01318-6>.
- Zhao Y, Wang Q, Liu H et al. High-throughput sequencing of 16S rRNA amplicons characterizes gut microbiota shift of juvenile sea cucumber *Apostichopus japonicus* feeding with three antibiotics. *J Ocean Limnol* 2019;**37**:1714–25. <https://doi.org/10.1007/s00343-019-8308-5>.
- Zou S, Zhang Q, Zhang X et al. Environmental factors and pollution stresses selected bacterial populations in association with protists. *Front Mar Sci* 2020;**7**:659. <https://doi.org/10.3389/fmars.2020.00659>.

Received 24 April 2025; revised 9 July 2025; accepted 29 July 2025

© The Author(s) 2025. Published by Oxford University Press on behalf of FEMS. This is an Open Access article distributed under the terms of the Creative Commons Attribution-NonCommercial License (<https://creativecommons.org/licenses/by-nc/4.0/>), which permits non-commercial re-use, distribution, and reproduction in any medium, provided the original work is properly cited. For commercial re-use, please contact reprints@oup.com for reprints and translation rights for reprints. All other permissions can be obtained through our RightsLink service via the Permissions link on the article page on our site—for further information please contact journals.permissions@oup.com.